

Development of a fully coupled flow-geomechanics simulator for flow in saturated porous media

†*Chao Zhang, Sadiq J. Zarrouk and Rosalind Archer

Department of Engineering Science
University of Auckland, Private Bag 92019, Auckland, New Zealand

*Presenting author: chao.zhang@auckland.ac.nz
†Corresponding author: chao.zhang@auckland.ac.nz

Abstract

In this paper, we propose a fully coupled flow-geomechanics simulator using the mixed finite element method. The mathematical model, including mass conservation of fluid, Darcy's law for velocity, and force equilibrium of solid skeleton, is derived in the framework of Biot's consolidation theory. Pore pressure, fluid velocity and solid displacement are chosen as primary variables. This has the advantage of satisfying element-wise mass conservation and describing the velocity in a continuous way, instead of as a derived value of pressure, as in traditional simulators. The mathematical model is then discretized in appropriate finite element spaces. Specifically, we use the constant discontinuous Galerkin space for pressure, the lowest order Brezzi-Douglas-Marini space for fluid velocity, and the linear Continuous Galerkin space for solid displacement. The system of equations is solved in a fully coupled manner, which ensures second order convergence and stability. Afterwards, the resulted model is validated using a wide range of benchmark problems, including the consolidation problems of Terzaghi, Mandel and Cryer. In all cases, our numerical results are in good agreement with the analytical solutions, which illustrates the effectiveness of our simulator, especially in capturing the Mandel-Cryer effect accurately.

Keywords: Mixed finite element, Poro-elasticity, Consolidation, Fully-coupled model, Porous media

Introduction

In many applications involving porous media, it is of paramount importance to model the interaction between fluid flow and solid deformation in a tightly coupled manner to make accurate predications [Gambolati et al., 1991; Pao et al., 2001; Teatini et al., 2006; Yin et al., 2009]. This paper will focus on developing an alternative simulator to accurately describe this coupled process.

From the mathematics point of view, the mutual coupling between fluid flow and solid deformation leads to a complex initial-boundary-value problem. Over the past decades, a lot of researchers have studied this problem through different numerical methods, namely the finite difference method [Lee et al., 1998; Masson and Pride, 2007; Yanosik et al., 1979], the finite element method [Edwards, 2002; Lewis and Schrefler, 1987; Panneton and Atalla, 1997; Wheeler et al., 2014], and the finite volume method [Jenny et al., 2005; Mosharaf Dehkordi et al., 2014; Rozon et al., 1989]. Compared with the finite difference method and the finite volume method, not only could the finite element method handle well complex geometries, which is common in reservoir simulations, it is also good at multiple field problems [Fortin and Brezzi, 1991; Hesthaven and War-

burton, 2007].

In the literature, there are three coupling approaches (explicitly coupled, iteratively coupled and fully coupled) to study the fluid-solid interaction problem. In the explicitly coupled approach [Longuemare et al., 2002; Minkoff et al., 2003], the flow variables are assumed constant when solving the force equilibrium equation, and vice versa. This method requires relatively small time steps to ensure a physical solution. In the iteratively coupled scheme [Mikelić and Wheeler, 2013; Tran et al., 2004], each simulator solves its own governing equation and uses some correction terms to make sure that the equations are solved at the same time step. Since the coupled problem is split into a flow problem and a solid deformation problem, it results in two much smaller problems and saves computational time. Although an iterative method has the advantage of efficiency, the disadvantage is that it may introduce splitting errors. Especially in gas flow cases, splitting error may lead to unphysical solutions [Aarnes et al., 2007]. A third method is to solve the coupled flow and solid system simultaneously, which is referred to as the fully coupled approach [Khoshghalb and Khalili, 2010; Settari et al., 1998; White and Borja, 2011]. In this approach, each equation is discretized implicitly, which guarantees its robustness. However, the disadvantage is also obvious: it results in a larger system of equations and may require more computational time.

In this work, we present a fully coupled solver to account for the interaction between fluid flow and geomechanics by the finite element method. The mathematical model is proposed based on Biot's theory in poromechanics, and a subsequent numerical model is implemented by the mixed finite element techniques. Specifically, we use the lowest order Brezzi-Douglas-Marini function space (BDM1) and the constant Discontinuous Galerkin function space (DG0) for the fluid velocity and pressure field, respectively. This pair of function spaces ensures local mass conservation, which is relatively important in flow related problems. As to the solid displacement field, the standard linear Continuous Galerkin interpolant is used. The related system is then solved in a fully coupled manner, which ensures second order convergence.

In the following sections, we will show all the aspects in developing the flow-geomechanics simulator. Specifically, in Section 2 we briefly outline the mathematical equations used in this coupled problem. Section 3 discusses the weak form derivation, space and time discretization and finite element implementation. Section 4 examines the correctness of the developed solver by comparing the numerical results with some classic benchmark problems. Finally in Section 5, we draw conclusions.

Mathematical Model

Governing equations

As in classic continuum mechanics, the whole system is viewed as a number of overlapping continua representing the corresponding phase, namely solid skeleton and fluid. The representative elementary volume (REV) is large enough to preserve the physical properties, like porosity and permeability. On the other hand, the REV must be sufficiently small to be considered as a point in the macroscopic scale.

In the framework of Biot [1941] poromechanics, we make the following assumptions: (1) the pore water is incompressible, (2) the solid grains are incompressible, (3) small

strain theory is applicable, (4) the soil as a whole exhibit linear elastic deformation, and (5) the system is isothermal.

The flow of fluid through the porous medium is described by the mass conservation equation as:

$$\frac{\partial}{\partial t}(\nabla \cdot \mathbf{u}_s) + \nabla \cdot \mathbf{u} = f_f, \quad (1)$$

where \mathbf{u}_s is solid skeleton displacement, \mathbf{u} is fluid velocity relative to solid skeleton, and f_f is fluid source term.

The relative velocity of fluid \mathbf{u} is usually governed by the Darcy's law as:

$$\mathbf{u} + \frac{\mathbf{k}}{\mu} \nabla p = 0, \quad (2)$$

where p is fluid pressure, and \mathbf{k} is permeability tensor, and μ is dynamic viscosity. In simplified cases, isotropy can be assumed in porous media, and the corresponding permeability tensor is a diagonal one. By nature, most porous media systems are directionally dependent, and thus a full tensor permeability is usually more appropriate to accurately describe the flow path.

As we assume the system is quasi-static, the equation of force equilibrium can be expressed in terms of the total stress as:

$$\nabla \boldsymbol{\sigma} + \mathbf{f}_s = 0, \quad (3)$$

where $\boldsymbol{\sigma}$ is total stress, and \mathbf{f}_s is body force, i.e. gravity. The relation between total stress $\boldsymbol{\sigma}$, effective stress $\boldsymbol{\sigma}_e$, and fluid pressure p is given as:

$$\boldsymbol{\sigma} = \boldsymbol{\sigma}_e - \alpha p \mathbf{I}, \quad (4)$$

where \mathbf{I} is the identity matrix, and α is the Biot coefficient. The sign convention, namely that positive stress is taken as tension and negative compression, is applied here.

The constitutive equation relating the effective stress to strain $\boldsymbol{\varepsilon}$ reads:

$$\boldsymbol{\sigma} = 2G\boldsymbol{\varepsilon} + \lambda\varepsilon_v \mathbf{I}, \quad (5)$$

where ε_v is the volumetric strain, G and λ are Lamé constants.

By applying the small strain theory, strain is related to the solid skeleton displacement as:

$$\boldsymbol{\varepsilon} = \frac{1}{2}[\nabla \mathbf{u}_s + (\nabla \mathbf{u}_s)^T]. \quad (6)$$

Initial and boundary conditions

In order to complete the coupled equation system, we need to apply suitable initial and boundary conditions for both the fluid and solid part.

Initially, we assume that fluid pressure, fluid velocity, and solid displacements are known values as:

$$\begin{cases} p = p^0 \\ \mathbf{u} = \mathbf{u}^0 \\ \mathbf{u}_s = \mathbf{u}_s^0 \end{cases} \quad \text{in } \Omega, \quad (7)$$

at $t = 0$.

When $t > 0$, we consider the following boundary condition for the solid problem:

$$\begin{cases} \mathbf{u}_s = \mathbf{u}_s^b, & \text{on } \Gamma_{u_s} \\ \boldsymbol{\sigma} \mathbf{n} = \mathbf{g}, & \text{on } \Gamma_\sigma \end{cases}, \quad (8)$$

where \mathbf{n} denotes unit outward normal vector of the boundary, and \mathbf{g} is boundary force. As to the fluid flow part, the following boundary conditions are applied:

$$\begin{cases} p = p^b, & \text{on } \Gamma_p \\ \mathbf{u} = \mathbf{u}^b, & \text{on } \Gamma_u \end{cases}. \quad (9)$$

Γ_p , Γ_u , Γ_{u_s} and Γ_σ are corresponding pressure, velocity, displacement and exterior stress boundaries.

Before concluding this section, we summarize the three governing equations described above:

$$\frac{\partial}{\partial t}(\nabla \cdot \mathbf{u}_s) + \nabla \cdot \mathbf{u} = f_f, \quad (10)$$

$$\mathbf{u} + \frac{\mathbf{k}}{\mu} \nabla p = 0, \quad (11)$$

$$\nabla \boldsymbol{\sigma} + \mathbf{f}_s = 0. \quad (12)$$

Numerical Implementation

Weak form derivation

We consider this problem posed on the physical domain Ω with boundary $\partial\Omega$. Let triangulation $\mathcal{T}_h = \{K\}$ be a partition of the domain Ω , and K is a subset of Ω . In order to perform finite element discretization, we need to introduce suitable function spaces for the test and trial functions. We set

$$L^2(\Omega) = \{p : \int_{\Omega} |p|^2 dx < +\infty\}, \quad (13)$$

$$H^1(\Omega) = \{u : u \in L^2(\Omega), Du \in L^2(\Omega)\}, \quad (14)$$

$$H(\text{div}, \Omega) = \{\mathbf{v} : \mathbf{v} \in L^2(\Omega)^d, \nabla \cdot \mathbf{v} \in L^2(\Omega)\}. \quad (15)$$

Fluid pressure must belong to $L^2(\Omega)$, fluid velocity belongs to $H^1(\Omega)^d$ and solid displacement belongs to $H(\text{div}, \Omega)$, respectively. d denotes the number of space dimensions.

Multiplying Equation (10), Equation (11), Equation (12) by test functions q , \mathbf{v} and \mathbf{v}_s , respectively, and integrating by parts on Ω , we get the following residual formulation: Find $p \in L^2(\Omega)$, $\mathbf{u} \in H^1(\Omega)$ and $\mathbf{u}_s \in H(\text{div}, \Omega)$ such that we have

$$\mathcal{R}_p = \int_{\Omega} \frac{\partial}{\partial t} (\nabla \mathbf{u}_s) q \, dx + \int_{\Omega} \nabla \cdot \mathbf{u} q \, dx - \int_{\Omega} f_f q \, dx = 0, \quad (16)$$

$$\mathcal{R}_u = \int_{\Omega} \mathbf{u} \cdot \mathbf{v} \, dx - \int_{\Omega} \frac{\mathbf{k}}{\mu} p \nabla \cdot \mathbf{v} \, dx + \int_{\Gamma} \frac{\mathbf{k}}{\mu} p \mathbf{v} \cdot \mathbf{n} \, ds = 0, \quad (17)$$

$$\mathcal{R}_{u_s} = \int_{\Omega} \boldsymbol{\sigma} \nabla \cdot \mathbf{v}_s \, dx - \int_{\Gamma} \mathbf{n} \cdot \boldsymbol{\sigma} \mathbf{v}_s \, ds - \int_{\Omega} \mathbf{f}_s \mathbf{v}_s \, dx = 0, \quad (18)$$

for all $q \in L^2(\Omega)$, $\mathbf{v} \in H^1(\Omega)$ and $\mathbf{v}_s \in H(\text{div}, \Omega)$. The symbol \mathcal{R} refers to residual.

Space and time discretization

Fluid pressure p , fluid velocity \mathbf{u} and solid displacement \mathbf{u}_s are chosen as primary variables, as indicated earlier in this paper. In order to make the problem well-posed, the function spaces and the polynomial degrees of shape functions for the pressure and the velocity can not be chosen arbitrarily [Fortin and Brezzi, 1991]. Instead, a pair of finite element spaces that satisfy the in-sup condition is required. In this study, we choose the elementwise constant space (DG0) for pressure, the lowest order Brezzi-Douglas-Marini space (BDM1) for fluid velocity, and the linear Continuous Galerkin space (CG1) for solid displacement.

Compared with the standard finite element method, the advantages of this mixed form are: (1) it satisfies element-wise mass conservation, (2) the stability and convergence are ensured, (3) it avoids the numerical diffusion in standard finite element method, and (4) the velocity is described in a continuous way, instead of as a derived value of pressure.

We interpolate pressure, velocity and displacement in the discretized space as:

$$p_h = \sum_{i=1}^{n_{elem}} \phi_i P_i \quad (19)$$

$$\mathbf{u}_h = \sum_{i=1}^{n_{face}} \phi_i \mathbf{U}_i \quad (20)$$

$$\mathbf{u}_{sh} = \sum_{i=1}^{n_{node}} \phi_i \mathbf{U}_{s_i} \quad (21)$$

where p_h , \mathbf{u}_h and \mathbf{u}_{sh} are discrete variables, ϕ is shape function, and P , \mathbf{U} and \mathbf{U}_s are values at corresponding elements, faces and nodes. n_{elem} , n_{face} and n_{node} are respective numbers of elements, faces and nodes.

As for time discretization, we apply the conventional backward Euler scheme, which ensures first order accuracy:

$$\frac{\partial}{\partial t}(\nabla \mathbf{u}_s) = \frac{\nabla \mathbf{u}_s - \nabla \mathbf{u}_{s0}}{\Delta t} \quad (22)$$

where Δt is time step.

Coupling scheme

As declared in the introduction section, the fully coupled scheme has the advantage of ensuring stability and avoids convergence issues. Therefore, the fully coupled approach is employed in our model. Specifically, all the three equations are solved simultaneously at each time step, and the implicit Newton-Raphson method is used to update the solution. At time step $(n + 1)$, the solution at $(k + 1)$ th iteration is updated by adding the correction terms to the solution at k th iteration as:

$$\begin{bmatrix} p^{n+1} \\ \mathbf{u}^{n+1} \\ \mathbf{u}_s^{n+1} \end{bmatrix}^{k+1} = \begin{bmatrix} p^{n+1} \\ \mathbf{u}^{n+1} \\ \mathbf{u}_s^{n+1} \end{bmatrix}^k + \begin{bmatrix} \delta p^{n+1} \\ \delta \mathbf{u}^{n+1} \\ \delta \mathbf{u}_s^{n+1} \end{bmatrix}, \quad (23)$$

where the correction comes from solving the following linear system:

$$\begin{bmatrix} \frac{\partial \mathcal{R}_p}{\partial p} & \frac{\partial \mathcal{R}_p}{\partial \mathbf{u}} & \frac{\partial \mathcal{R}_p}{\partial \mathbf{u}_s} \\ \frac{\partial \mathcal{R}_u}{\partial p} & \frac{\partial \mathcal{R}_u}{\partial \mathbf{u}} & \frac{\partial \mathcal{R}_u}{\partial \mathbf{u}_s} \\ \frac{\partial \mathcal{R}_{u_s}}{\partial p} & \frac{\partial \mathcal{R}_{u_s}}{\partial \mathbf{u}} & \frac{\partial \mathcal{R}_{u_s}}{\partial \mathbf{u}_s} \end{bmatrix} \begin{bmatrix} \delta p^{n+1} \\ \delta \mathbf{u}^{n+1} \\ \delta \mathbf{u}_s^{n+1} \end{bmatrix} = \begin{bmatrix} \mathcal{R}_p \\ \mathcal{R}_u \\ \mathcal{R}_{u_s} \end{bmatrix}, \quad (24)$$

and the symbol δ denotes correction.

Implementation in FEniCS

We create our code based on the recently developed open source project, FEniCS [Logg et al., 2012], which is a collection of libraries to facilitate the automated solution of partial differential equations using finite element method.

Numerical Tests

In this section, we test the performance of the developed solver by solving a series of benchmark problems.

Terzaghi's 1D problem

The first example involves the consolidation problem from Terzaghi [1996], as illustrated in Figure 1. In this 1D problem, the top surface is assumed to be fully drained, while the bottom surface is impermeable. As for the solid part, the top surface is exposed to a constant vertical load and the bottom face is fixed. The length of the beam is taken as $L = 15$ m, and other parameters are summarized in Table 1.

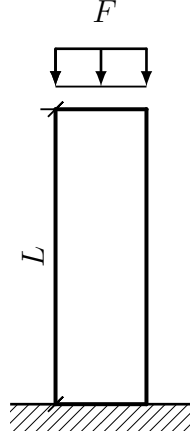


Figure 1: Sketch of Terzaghi's 1D problem.

Table 1: Parameters in Terzaghi's problem

Parameter	Value
Young's modulus	100.0 <i>MPa</i>
Poisson's ratio	0.25
Biot coefficient	1.0
Overload	1000.0 <i>Pa</i>
Permeability	$1.0e^{-14}$ <i>m</i> ²
Dynamic viscosity	$1.0e^{-5}$ <i>m</i> ² / <i>sec</i>
Time step length	$1.0e^{-3}$ <i>sec</i>
Column length	15.0 <i>m</i>

The analytical solution is given by Verruijt [2013] through Laplace transformation:

$$\bar{p} = \frac{4}{\pi} \sum_{k=1}^{\infty} \cos\left[(2k-1)\frac{\pi}{2}\bar{x}\right] \exp\left[-(2k-1)^2\frac{\pi^2}{4}\bar{t}\right], \quad (25)$$

where \bar{p} is normalized pressure $\frac{p}{p_0}$, \bar{x} is normalized distance $\frac{x}{L}$, \bar{t} is normalized time $\frac{c_v t}{h^2}$, and c_v is consolidation coefficient.

Our numerical results are shown in Figure 2 and Figure 3. It can be observed from Figure 2 that the agreement between our numerical result and the analytical solution appears excellent. At time $t = 0$, a constant load is applied to the top surface. This sudden increase in load will be initially suffered by the water, and thus the water pressure goes up everywhere in the beam. The pore pressure then gradually vanishes, since the top surface is fully drained. This dissipation process may take considerable time, depending on the permeability value.

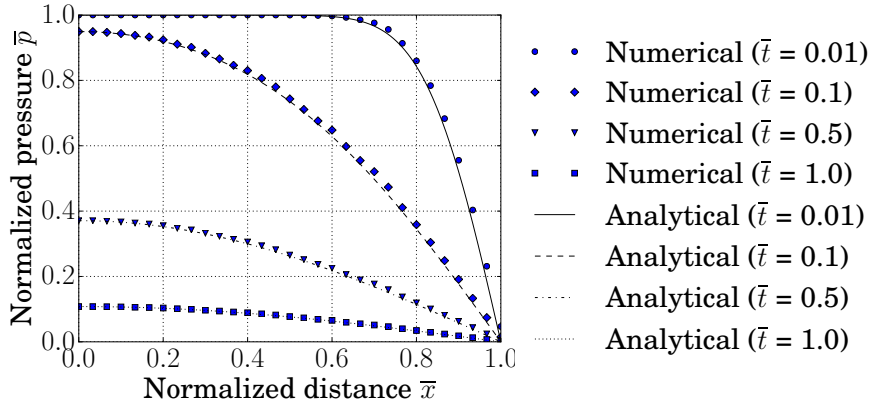


Figure 2: Comparison of the numerical and analytical solutions of Terzaghi's problem: excess pore pressure at different normalized time.

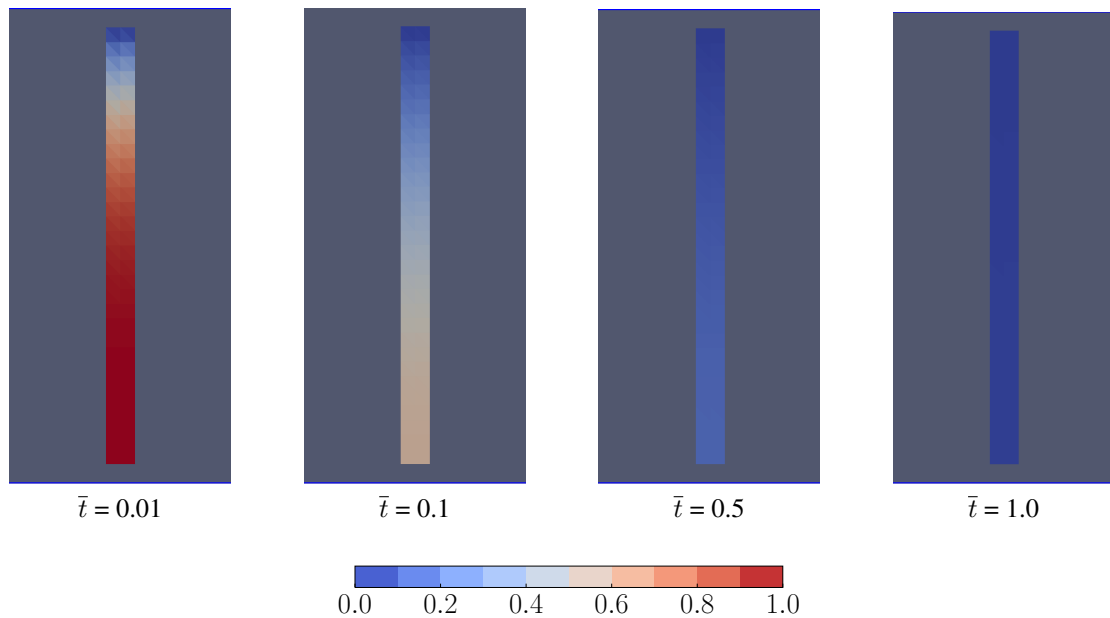


Figure 3: Normalized pressure distribution of Terzaghi's problem at different normalized time

Mandel's 2D problem

In this example, we consider the 2D consolidation problem from Mandel [1953]. As illustrated in Figure 4, a rectangular soil sample is sandwiched between rigid frictionless plates at its top and bottom. The top and bottom surface are impermeable and the lateral surfaces are allowed to drain freely. The length and width of the sample are $2L_1 = 2$ m and $2L_2 = 2$ m, respectively. Other physical and computational parameters are given in Table 2.

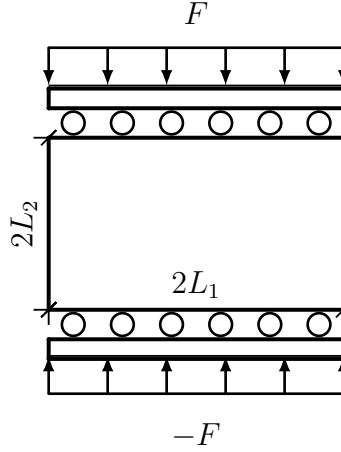


Figure 4: Sketch of Mandel's problem.

Table 2: Parameters in Mandel's problem

Parameter	Value
Young's modulus	100.0 MPa
Poisson's ratio	0.25
Biot coefficient	1.0
Overload	1000.0 Pa
Permeability	$1.0e^{-14} m^2$
Dynamic viscosity	$1.0e^{-5} m^2/s$
Time step length	$1.0e^{-3} s$
Plate length	1.0 m
Plate width	1.0 m

The analytical solution is given by Abousleiman et al. [1996] and Coussy [2004] as:

$$\bar{p} = 2 \sum_{k=1}^{\infty} \frac{\cos(\alpha_k \bar{x}) - \cos \alpha_k}{\alpha_k - \sin \alpha_k \cos \alpha_k} \exp(-\alpha_n^2 \bar{t}), \quad (26)$$

where α_k is the solution of:

$$\frac{\tan \alpha_k}{\alpha_n} = \frac{1 - v}{v_n - v}, \quad (27)$$

and v_n and v stands for undrained and drained Poisson ration, respectively. For incompressible constituents, v_n is 0.5.

The numerical results in terms of normalized pressure versus normalized time are presented in Figure 5 and Figure 6. Similar to Terzaghi's 1D problem, the pressure jumps to some value and then gradually dissipates. It is important to note that the pressure at the centre of plate continues to increase after its initial creation by the Skempton effect [Skempton, 1954]. This is due to the fact that the generation of pore pressure is immediate, but the dissipation caused by the fluid flow is delayed by the small permeability and the flow path to escape from the lateral boundaries.

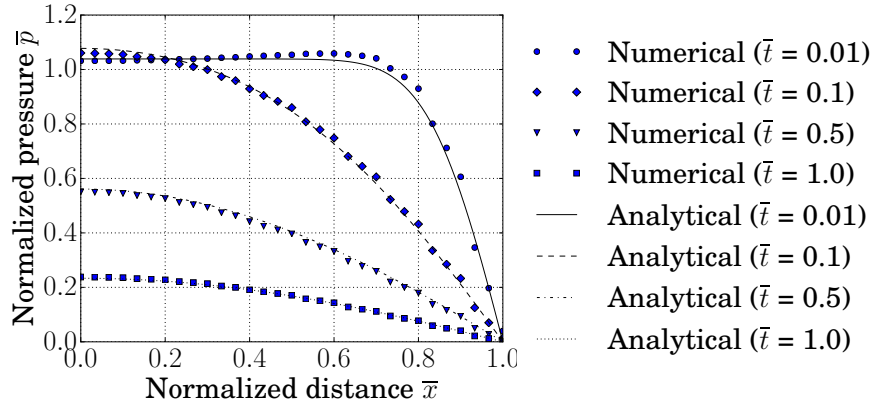


Figure 5: Comparison of the numerical and analytical solutions of Mandel’s problem: excess pore pressure at different normalized time.

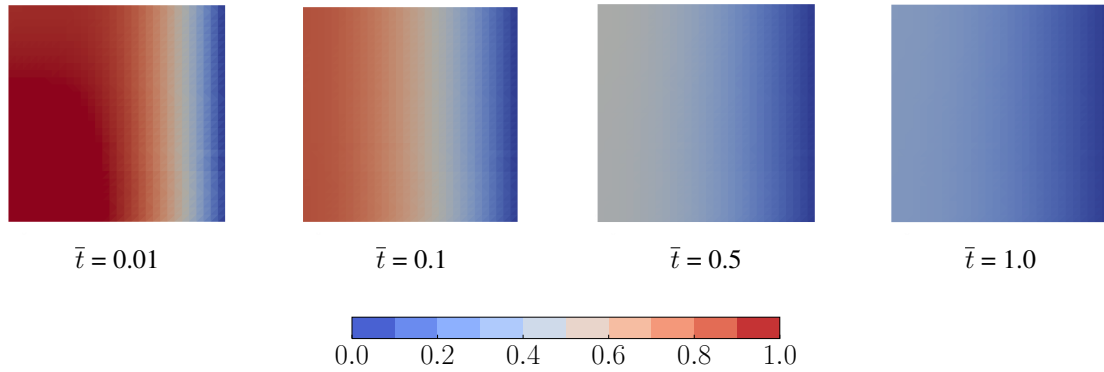


Figure 6: Normalized pressure distribution of Mandel’s problem at different normalized time

Cryer’s 3D problem

Finally, we consider the sphere from Cryer [1963], a classic 3D consolidation problem. In this case, a 3D spherical soil sample, of radius $a = 1.0\text{ m}$, is loaded on its outer boundary by an instantaneous uniform confining pressure of magnitude F , see Figure 7. Table 3 summarizes all the useful parameters.

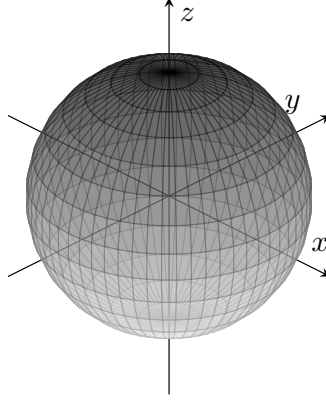


Figure 7: Sketch of Cryer's problem.

Table 3: Parameters in Cryer's problem

Parameter	Value
Young's modulus	10.0 MPa
Poisson's ratio	0.33
Biot coefficient	1.0
Overload	1000.0 Pa
Permeability	$4.95e^{-14} m^2$
Dynamic viscosity	$1.0e^{-5} m^2/s$
Time step length	$1.0e^{-2} s$
Sphere radius	1.0 m

We are interested in the pressure evolution at the centre of the sphere and the analytical solution is given by Verruijt [2013] as:

$$\bar{p} = \eta \sum_{k=1}^{\infty} \frac{\sin \alpha_k - \alpha_k}{\eta \alpha_k \cos \alpha_k / 2 + (\eta - 1) \sin \alpha_k} \exp(-\alpha_k^2 \bar{t}), \quad (28)$$

where α_k is the positive roots of the equation:

$$(1 - \eta \alpha_k^2) \tan \alpha_k = \alpha_k, \quad (29)$$

where η is defined as $\frac{\lambda + 2G}{2G}$.

We show the numerical results in Figure 8 and Figure 9. Initially when $t = 0$, the pressure at the centre jumps by an amount, and then continues to rise for a while before declining, as in the case of Mandel's problem. This non-monotonic pore pressure response, a rise in interior fluid pressure and the subsequent decaying to zero value, is referred to as the Mandel-Cryer effect. This is a distinctive phenomenon of Boit's consolidation, which is not observed by the traditional uncoupled theory [Terzaghi et al., 1943]. As shown in Figure 8, our model greatly captures the Mandel-Cryer effect.

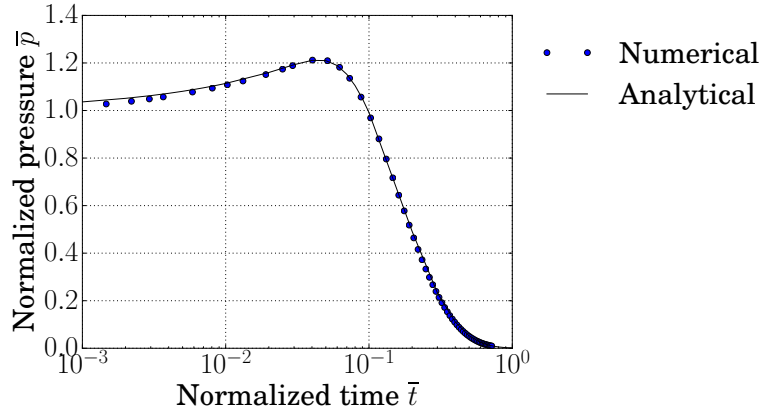


Figure 8: Comparison of the numerical and analytical solutions of Cryer’s problem: excess pore pressure at the center.

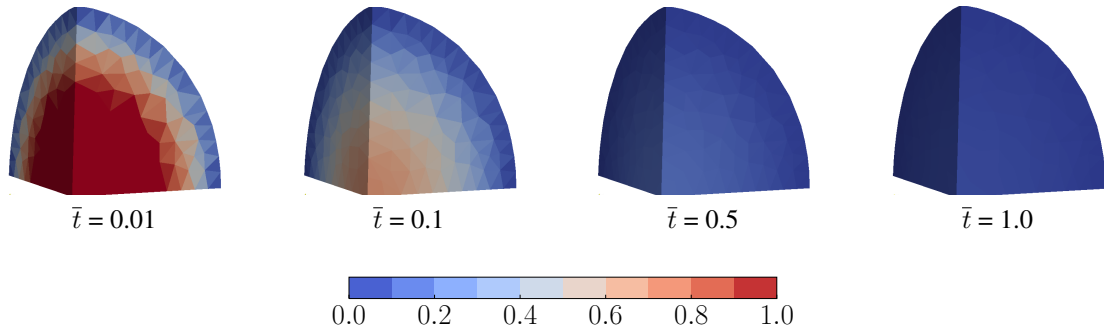


Figure 9: Normalized pressure distribution of Cryer’s problem at different normalized time

Conclusion

In this work, we have developed a fully coupled 3D model for flow-geomechanical simulation in porous media. By choosing fluid pressure, velocity and solid displacement as primary variables, the proposed mixed finite element formulation is able to ensure local mass conservation and express the velocity and displacement in a continuous way. The fully coupled approach is unconditionally stable, and eliminates the convergence issues encountered in explicit scheme and iterative coupled scheme. The performance of the resulting numerical model is validated according to Terzaghi’s 1D problem, Mandel’s 2D problem and Cryer’s 3D problem. In all cases, our numerical results show good agreement with the analytical solutions.

Acknowledgements

The authors wish to acknowledge the financial support from China Scholarship Council, and the contribution of the NeSI high-performance computing facilities and the eResearch centre at the University of Auckland. The first author would also like to express his gratitude to Dr. Jon Pearce for his invaluable help in developing the codes.

REFERENCES

- Aarnes, Jørg E, Tore Gimse, and Knut-Andreas Lie. An introduction to the numerics of flow in porous media using matlab. In *Geometric modelling, numerical simulation, and optimization*, pages 265–306. Springer, 2007.
- Abousleiman, Y, AH-D Cheng, L Cui, E Detournay, and J-C Roegiers. Mandel’s problem revisited. *Geotechnique*, 46(2):187–195, 1996.
- Biot, Maurice A. General theory of three-dimensional consolidation. *Journal of applied physics*, 12(2):155–164, 1941.
- Coussy, Olivier. *Poromechanics*. John Wiley & Sons, 2004.
- Cryer, CW. A comparison of the three-dimensional consolidation theories of biot and terzaghi. *The Quarterly Journal of Mechanics and Applied Mathematics*, 16(4):401–412, 1963.
- Edwards, Michael G. Unstructured, control-volume distributed, full-tensor finite-volume schemes with flow based grids. *Computational Geosciences*, 6(3-4):433–452, 2002.
- Fortin, Michel and Franco Brezzi. *Mixed and hybrid finite element methods*. New York: Springer-Verlag, 1991.
- Gambolati, Giuseppe, Giuseppe Ricceri, Werter Berton, Giovanni Brighenti, and Enzo Vuillermin. Mathematical simulation of the subsidence of ravenna. *Water Resources Research*, 27(11):2899–2918, 1991.
- Hesthaven, Jan S and Tim Warburton. *Nodal discontinuous Galerkin methods: algorithms, analysis, and applications*, volume 54. Springer Science & Business Media, 2007.
- Jenny, P, SH Lee, and HA Tchelepi. Adaptive multiscale finite-volume method for multiphase flow and transport in porous media. *Multiscale Modeling & Simulation*, 3(1):50–64, 2005.
- Khoshghalb, Arman and Nasser Khalili. A stable meshfree method for fully coupled flow-deformation analysis of saturated porous media. *Computers and Geotechnics*, 37(6):789–795, 2010.
- Lee, SH, LJ Durlofsky, MF Lough, WH Chen, and others. Finite difference simulation of geologically complex reservoirs with tensor permeabilities. *SPE Reservoir Evaluation and Engineering*, 1(6):567–574, 1998.
- Lewis, Roland Wynne and Bernard A Schrefler. *The finite element method in the deformation and consolidation of porous media*. 1987.
- Logg, Anders, Kent-Andre Mardal, and Garth Wells. *Automated solution of differential equations by the finite element method: The FEniCS book*, volume 84. Springer Science & Business Media, 2012.
- Longuemare, P, M Mainguy, P Lemonnier, A Onaisi, Ch Gérard, and N Koutsabeloulis. Geomechanics in reservoir simulation: overview of coupling methods and field case study. *Oil & Gas Science and Technology*, 57(5):471–483, 2002.
- Mandel, J. Consolidation des sols (étude mathématique)*. *Geotechnique*, 3(7):287–299, 1953.
- Masson, Yder J and Steven R Pride. Poroelastic finite difference modeling of seismic attenuation and dispersion due to mesoscopic-scale heterogeneity. *Journal of Geophysical Research: Solid Earth (1978–2012)*, 112(B3), 2007.

- Mikelić, Andro and Mary F Wheeler. Convergence of iterative coupling for coupled flow and geomechanics. *Computational Geosciences*, 17(3):455–461, 2013.
- Minkoff, Susan E, C Mike Stone, Steve Bryant, Malgorzata Peszynska, and Mary F Wheeler. Coupled fluid flow and geomechanical deformation modeling. *Journal of Petroleum Science and Engineering*, 38(1):37–56, 2003.
- Mosharaf Dehkordi, Mehdi, Mehrdad T. Manzari, H Ghafouri, and R Fatehi. A general finite volume based numerical algorithm for hydrocarbon reservoir simulation using blackoil model. *International Journal of Numerical Methods for Heat & Fluid Flow*, 24(8):1831–1863, 2014.
- Panneton, Raymond and Noureddine Atalla. An efficient finite element scheme for solving the three-dimensional poroelasticity problem in acoustics. *The Journal of the Acoustical Society of America*, 101(6):3287–3298, 1997.
- Pao, William KS, Roland W Lewis, and Ian Masters. A fully coupled hydro-thermo-poro-mechanical model for black oil reservoir simulation. *International journal for numerical and analytical methods in geomechanics*, 25(12):1229–1256, 2001.
- Rozon, Brad J and others. A generalized finite volume discretization method for reservoir simulation. In *SPE Symposium on Reservoir Simulation*. Society of Petroleum Engineers, 1989.
- Settari, Antonin, FM Mourits, and others. A coupled reservoir and geomechanical simulation system. *Spe Journal*, 3(03):219–226, 1998.
- Skempton, AW. The pore-pressure coefficients a and b. *Geotechnique*, 4(4):143–147, 1954.
- Teatini, P, M Ferronato, G Gambolati, and M Gonella. Groundwater pumping and land subsidence in the emilia-romagna coastland, italy: Modeling the past occurrence and the future trend. *Water Resources Research*, 42(1), 2006.
- Terzaghi, Karl. *Soil mechanics in engineering practice*. John Wiley & Sons, 1996.
- Terzaghi, Karl, Karl Terzaghi, Civil Engineer, Austria Czechoslovakia, Karl Terzaghi, Ingénieur Civil, Autriche Tchecoslovaquie, and Etats Unis. *Theoretical soil mechanics*, volume 18. Wiley New York, 1943.
- Tran, David, Antonin Settari, Long Nghiem, and others. New iterative coupling between a reservoir simulator and a geomechanics module. *SPE Journal*, 9(03):362–369, 2004.
- Verruijt, Arnold. Theory and problems of poroelasticity. *Delft University of Technology*, 2013.
- Wheeler, Mary, Guangri Xue, and Ivan Yotov. Coupling multipoint flux mixed finite element method with continuous galerkin methods for poroelasticity. *Computational Geosciences*, 18(1):57–75, 2014.
- White, Joshua A and Ronaldo I Borja. Block-preconditioned newton–krylov solvers for fully coupled flow and geomechanics. *Computational Geosciences*, 15(4):647–659, 2011.
- Yanosik, JL, TA McCracken, and others. A nine-point, finite difference reservoir simulator for realistic prediction of adverse mobility ratio displacements. *Soc. Pet. Eng. J*, 19(4):253–262, 1979.
- Yin, Shunde, Maurice B Dusseault, and Leo Rothenburg. Thermal reservoir modeling in petroleum geomechanics. *International journal for numerical and analytical methods in geomechanics*, 33(4):449–485, 2009.